



EUROfusion

EUROFUSION WPHCD-PR(16) 15690

I.Gr. Pagonakis et al.

Multistage depressed collector conceptual design for thin magnetically confined electron beams

Preprint of Paper to be submitted for publication in
Physics of Plasmas



This work has been carried out within the framework of the EUROfusion Consortium and has received funding from the Euratom research and training programme 2014-2018 under grant agreement No 633053. The views and opinions expressed herein do not necessarily reflect those of the European Commission.

This document is intended for publication in the open literature. It is made available on the clear understanding that it may not be further circulated and extracts or references may not be published prior to publication of the original when applicable, or without the consent of the Publications Officer, EUROfusion Programme Management Unit, Culham Science Centre, Abingdon, Oxon, OX14 3DB, UK or e-mail Publications.Officer@euro-fusion.org

Enquiries about Copyright and reproduction should be addressed to the Publications Officer, EUROfusion Programme Management Unit, Culham Science Centre, Abingdon, Oxon, OX14 3DB, UK or e-mail Publications.Officer@euro-fusion.org

The contents of this preprint and all other EUROfusion Preprints, Reports and Conference Papers are available to view online free at <http://www.euro-fusionscipub.org>. This site has full search facilities and e-mail alert options. In the JET specific papers the diagrams contained within the PDFs on this site are hyperlinked

Multistage depressed collector conceptual design for thin magnetically confined electron beams

Ioannis Gr. Pagonakis,¹ Chuanren Wu,¹ Stefan Illy,¹ and John Jelonnek¹

¹*Karlsruhe Institute of Technology (KIT), IHM, 76131 Karlsruhe, Germany*

The requirement of higher efficiency in high power microwave devices, such as traveling wave tubes and gyrotrons, guides scientific research to more advanced types of collector systems. First, a conceptual design approach of a multistage depressed collector for a sheet electron beam confined by a magnetic field is presented. The sorting of the electron trajectories according to their initial kinetic energy, is based on the $\mathbf{E} \times \mathbf{B}$ drift concept. The optimization of the geometrical parameters is based on analytical equations under several general assumptions. The analysis predicts very high levels of efficiency. Then, a design approach for the application of this type of collector to a gyrotron cylindrical hollow electron beam is also presented with very high levels of efficiency more than 80%.

PACS numbers: 34,323

I. INTRODUCTION

ECRH has become a well-established heating method for both tokamaks and stellarators [1]. As fusion machines become larger and operate at higher magnetic fields $B \approx 5 - 6$ T and higher plasma densities in steady state, it is necessary to develop very efficient CW gyrotrons that operate at both higher frequencies and higher mm-wave output powers.

In gyrotrons, typically an electronic efficiency η_e of up to about 35 to 40 % can be achieved. Consequently, after the interaction a significant amount of energy remains in the electron beam. An enhancement of the overall efficiency is achieved by energy recovery in a depressed collector. The kinetic energy of the electron beam after the interaction with the RF-field in the cavity is partly converted into electric energy, thus reducing the power consumption of the tube and increasing the overall efficiency η_t of the device.

The relation between the overall and the collector efficiency η_c which is defined by the fraction of spent electron beam energy converted to electrostatic energy, is given by the equation $\eta_t = \eta_e \eta_l / (1 - \eta_c(1 - \eta_e))$, where η_l is the ratio of the power losses (ohmic and stray radiation) to the generated microwave power. Single-stage depressed collectors with efficiency of about 60% have been successfully used in gyrotrons, increasing the overall efficiency of the tube to above 50 % [2]. It is understood that a significant amount of energy is still transformed into heat on the collector wall.

It is possible to increase the efficiency further by using a Multi-stage Depressed Collector (MDC). A MDC design is based on the configuration of an appropriate electric field using a set of electrodes (stages) and a magnetic field so as to direct electrons of the highest energy to the electrode with the greatest negative potential, the electrons with the lowest energy to the electrode with the lowest negative potential and the electrons with intermediate energies to electrodes with intermediate voltages to maximize energy recovery.

Two concepts have been proposed for the efficient sort-

ing of the electrons on the electrodes appropriate for gyrotrons where a strong magnetic field confines the electron beam. The first one is based on the application of a strongly varied adiabatic field (using magnetic iron) so as to produce adiabatic and controlled non-adiabatic electron trajectories. This approach has been patented by A. Singh et al. [3] since 1998. Several designs for MDCs based on this approach have been published since then [4–8] but a multi-stage depressed collector based on that concept has been never manufactured and experimentally tested.

The second concept for efficient sorting of the beam electron on the electrodes of a MDC was proposed for gyrotrons in 2008 [9]. The idea behind the proposed collector is based on the $\mathbf{E} \times \mathbf{B}$ drift. In particular, an electric field \mathbf{E} is generated by applying voltage to the electrodes in order to be at an angle to the magnetostatic field \mathbf{B} . The parallel component of the electric field E_{\parallel} is used, as usual, to decelerate the electrons. On the other hand, the transverse component of the electric field E_{\perp} , due to $\mathbf{E} \times \mathbf{B}$, causes a drift of the electrons perpendicular to the magnetic and electric fields. Under these conditions, the trajectory of the electrons is determined by the initial kinetic energy of the electrons at the entrance of the collector.

Two conceptual MDC designs for the gyrotron cylindrical hollow electron beam based on $\mathbf{E} \times \mathbf{B}$ have been published up to now. In the first one [9] a large number of electrodes with a very complex shape are used for the generation of the appropriate electric field with an axial and an azimuthal subcomponent. In order to fulfill the Faraday law, the azimuthal component of the generated electric field changes sign at two azimuthal angles (0 and 180 degrees). A MDC has been designed for the 2 MW, 170 GHz coaxial cavity gyrotron for ITER [10] for the demonstration of this idea with efficiency $\eta_c = 91$ % considering an infinite number of electrodes. Two important disadvantages of this approach are (i) the very complex electrode geometry and (ii) a possible thermal overload of the electrodes in the two azimuthal positions where the electric field changes direction and the concept is locally

invalid.

The second conceptual design based also on the $\mathbf{E} \times \mathbf{B}$ approach, in which a very simple geometry is considered, was presented very recently [11], i. The electrodes are axisymmetric coaxial rings placed along the axis which generate an axial decelerating electric field in the beam region. The magnetic field is defined with two subcomponents: an axial and an azimuthal one. The $\mathbf{E} \times \mathbf{B}$ drift, caused by the electric field and the azimuthal component of the magnetic field, produces a radial shift of the electrons outwards or inwards towards the outer or inner rings respectively, depending on the direction of the azimuthal component of the magnetic field. An overall gyrotron efficiency of 70-80% is demonstrated by simulation results for a system with four stages. However, it is very difficult or even impossible to generate the required magnetic field in gyrotrons as it is described in the paper in order to satisfy the Ampere-Maxwell law. A theoretically possible approach for the generation of such a magnetic field could be the application of a current on a coaxial insert at the inside of the electron beam which must be initiated from the gun of the gyrotron. This configuration will cause an azimuthal magnetic field in all parts of the gyrotron. Many difficulties are foreseen in the designs of the magnetron injection gun and the quasi-optical system in the presence of the azimuthal magnetic field and the coaxial structure.

It should also be mentioned that very recently we discovered in the bibliography that a MDC design based on $\mathbf{E} \times \mathbf{B}$ was proposed for TWT tubes since 1970 [12]. However, this idea was not attractive in such devices due to the fact that a simpler alternative approach based on electrostatic fields can be applied avoiding the additional complexity for the generation of the magnetic field required at the collector region.

In this work, a conceptual design approach for the efficient collection of a sheet beam based on the $\mathbf{E} \times \mathbf{B}$ is proposed and investigated in Sec. II. Then, in Sec. III an MDC design approach with simple electrode geometry for the gyrotron electron beam is also proposed which is based on two steps: (i) the transformation of the cylindrical hollow beam to a sheet beam using magnetostatic fields, and (ii) the collection of the sheet beam using the design presented in the first part of the paper. Simulation results using an upgraded version of the *Ariande* code [13] validate the proposed approach and a very high efficiency is predicted.

II. CONCEPTUAL DESIGN FOR A SHEET BEAM

The proposed MDC design consists of a set of N_e electrodes placed at an angle ϕ to a homogeneous magnetic field $\mathbf{B} = B\hat{\mathbf{z}}$, as conceptually shown in Fig. 1. Each electrode, except the last one, consists of two metallic rods placed parallel to each other at the axial position Z_i , symmetrically on the electron beam plane $y = 0$ at $y = Y_i$

and $y = -Y_i$, where $i = 1, \dots, N_e - 1$. The last electrode $i = N_e$ could be a bigger plate as is shown in Fig. 1. To each electrode a decelerating voltage $\Phi_{e,i}$ is applied, where $\Phi_{e,j} > \Phi_{e,j+1}$ for each $j = 1, \dots, N_e - 1$. In this way, an electric field $\mathbf{E} = E\hat{\mathbf{z}} = -d\Phi/dZ\hat{\mathbf{z}}$ is generated, with $E > 0$, at the beam plane $y = 0$, due to the symmetry of the electrodes and the monotonic decreasing of the voltages $\Phi_{e,i}$ along Z -axis. Assuming that the thickness of the electrodes in the Z direction is small, the above definition of the electric field can be considered valid in the entire region between the electrodes.

The electric field can be analyzed in two subcomponents: (i) the parallel to the magnetic field

$$E_z = -\cos(\phi) d\Phi/dZ$$

which decelerates the beam electrons, and (ii) the transverse

$$E_x = \sin(\phi) d\Phi/dZ,$$

which causes a drift velocity v_y for the electrons along y -axis, given by the equation

$$v_y = \frac{|\mathbf{E} \times \mathbf{B}|}{B^2} = \frac{-E_x}{B} = -\frac{\sin(\phi) d\Phi}{B dZ}. \quad (1)$$

pushing the beam electrons toward the electrodes.

Optimization and constraints

The optimal position of the electrodes and the efficiency are analytically calculated under several assumptions. Let us suppose that the kinetic energy distribution of the spent electron beam parallel to the magnetic field ranges between the values $\epsilon_{k,\min} = e\Phi_{0,\min}$ and $\epsilon_{k,\max} = e\Phi_{0,\max}$, where e is the absolute value of the

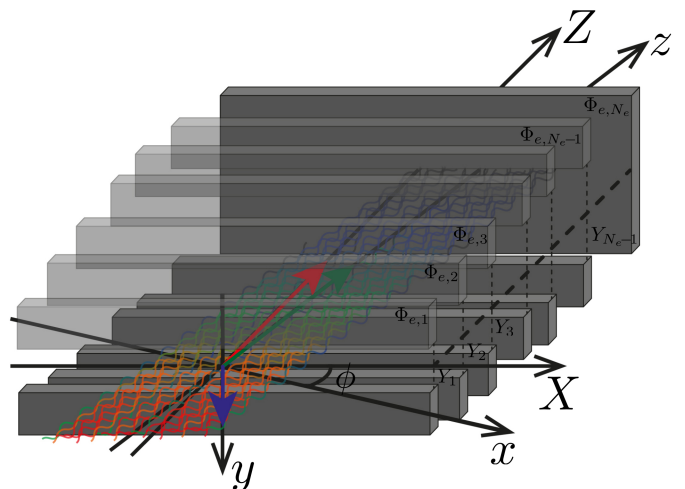


FIG. 1: Conceptual three-dimensional view of the sheet beam collector.

electron charge. The transverse energy is neglected, due to the fact that the part of the energy in the transverse direction cannot be recovered using the $\mathbf{E} \times \mathbf{B}$ concept. In order to minimize the efficiency reduction, a decompressing of the magnetic field before the collector is necessary for the transformation of the major part of the transverse energy to parallel energy.

The velocity of an electron inserted into the decelerating area at $Z = 0$ with an initial energy $e\Phi_0$ is written as

$$v_z(Z) = \pm \sqrt{\frac{2e}{m}(\Phi_0 + \Phi(Z))}$$

based on energy conservation, where m and e are the rest mass and the absolute value of the charge e of the electron. It is easy to show that the Z -component of the velocity can be written as $v_z(Z) = v_z(Z) \cos(\phi)$. Then, from the velocity definition we get

$$\frac{dY}{dZ} \equiv \frac{v_Y}{v_Z} = \mp \sqrt{\frac{m \tan(\phi)}{2e} \frac{d\Phi}{B} \frac{1}{\sqrt{\Phi_0 + \Phi(Z)}}} \quad (2)$$

and finally by integration we find that the Y -position of the electrons is a function only of the potential Φ which is expressed as

$$Y(\Phi) = Y_0 + \sqrt{\frac{2m \tan(\phi)}{e} \frac{1}{B}} \left[\sqrt{\Phi_0} \mp \sqrt{\Phi_0 + \Phi} \right] \quad (3)$$

where the "−" sign corresponds to the electron motion towards the positive z direction, while the "+" sign corresponds to the electron motion towards the negative z direction after a reflection due to the decelerating electric field.

Considering an infinitely thin beam $\Delta y \rightarrow 0$ and an infinite number of electrodes $N_e \rightarrow \infty$, the optimal position $Y_e(Z)$ of the electrodes is defined where the electron kinetic energy vanishes in the decelerating region, or $\Phi_0 = -\Phi(Z)$, which gives

$$Y_e(\Phi_0) = \frac{\tan(\phi)}{B} \sqrt{\frac{2m}{e} \Phi_0}. \quad (4)$$

The above equation shows that the optimal Y_e of any electrode depends only on the applied voltage and consequently it is independent of the variation of the electric field along the z -axis in beam region. In other words, the Z -positions of the electrodes do not influence the operation of the collector as long as the electrode Y_e positions satisfy eq. 4.

Using the substitutions $\nu = (-\Phi(Z)/\Phi_{0,\max})^{1/2}$ and $\psi = Y/Y_{\max}$ where

$$Y_{\max} = \frac{\tan(\phi)}{B} \sqrt{\frac{2m}{e} \Phi_{0,\max}} \quad (5)$$

eq. 3 is written as

$$\nu(\psi) = \sqrt{-\psi^2 + 2(\nu_0 + \psi_0)\psi - \psi_0(2\nu_0 + \psi_0)} \quad (6)$$

where $\nu_0 = (\Phi_0/\Phi_{0,\max})^{1/2}$ and $\psi_0 = Y_0/Y_{\max}$ are normalized quantities correlated with the initial kinetic energy and initial position along y , respectively. The optimal position of the electrodes given in eq. 4 is simplified as $\nu_c(\psi) = \psi$.

The trajectories of six sample electrons with different initial conditions (ψ_0, ν_0) in the phase space (ψ, ν) are plotted in Fig. 2. The electrons A , B and C were initiated at $\psi_0 = 0$ with energies $\nu_0 = 0.3, 0.6$ and 0.9 respectively. These electrons are gathered by the electrodes with zero velocity. This is not the case for all other electrons with $\psi_0 \neq 0$ in which a small amount of kinetic energy remains when their trajectories intersect the surface of the electrodes. Beam electrons with $\psi_0 > 0$, such as the electron E , are gathered before their energy vanishes due to the decelerating electric field. On the other hand, for electrons with $\psi_0 < 0$, such as the electrons D and F , their velocity first vanishes, and later on they are gathered while they are moving toward the collector entrance.

The normalized energy of the electrons when they are gathered by the electrodes placed along the line $\nu_c(\psi) = \psi$ is given by the equation

$$\nu_{c\pm}(\psi_0, \nu_0) = \frac{1}{2} \left(\nu_0 + \psi_0 \pm \sqrt{2\nu_0^2 - (\nu_0 + \psi_0)^2} \right). \quad (7)$$

Theoretically each electron trajectory intersects the electrode line at the two points with energies $\nu_c = \nu_{c+}$ and $\nu_c = \nu_{c-}$. In order to ensure high efficiency the electrons should be gathered when $\nu_c = \nu_{c+}$. However, all electrons are gathered before they reach the optimal electrode position. In particular, the trajectories of the beam electrons with $\psi_0 = 0$ intersect the line $\nu_c(\psi_0) = \psi_0$ at the entrance of the collector, the electrons with $\psi_0 > 0$ are gathered with energy ν_{c-} , while the electrons with $\psi_0 < 0$ are collected by the electrodes placed along the line $\nu_c(\psi_0) = -\psi_0$.

In order to ensure that the beam is inserted into the decelerating region and that all beam electrons will be gathered by the appropriate electrodes, several constraints are introduced. A visualization of the constraints is possible using Fig. 3, where a contour-plot of the final energy of the beam electrons when they are collected by the elec-

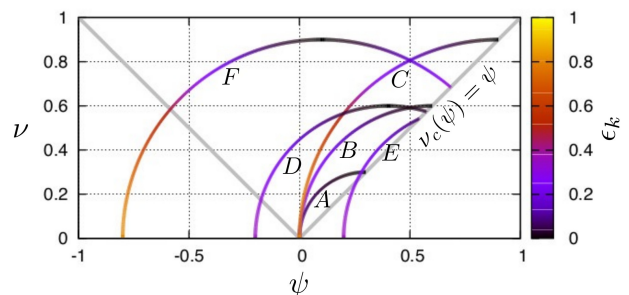


FIG. 2: The trajectories of six sample electrons in the phase space (ψ, ν) .

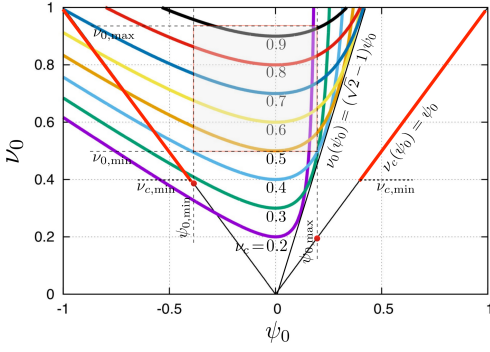


FIG. 3: Phase space of the initial electron beam properties and constraints for the optimal design.

trodes, given by eq. 7, is presented in the phase space of the initial properties (ψ_0, ν_0) . The initial properties of any beam can be represented in Fig 3 as a rectangle, vertically bounded by $\psi_{0,\min}$ and $\psi_{0,\max}$ and horizontally by $\nu_{0,\min}$ and $\nu_{0,\max}$. In the same figure, the optimal position of the electrodes is also plotted. Then, the constraints which ensure the compatibility of the collector with the initial beam properties are determined as follows:

- To ensure that the beam is inserted in the decelerating region one needs $\psi_{0,\min} > \nu_{c,\min}$ and $\psi_{0,\max} < (\sqrt{2} - 1)\nu_{0,\min}$ or equivalent; the rectangle defining the beam initial conditions (see Fig 3) should be to the right of the line $\nu_c(\psi_0) = -\psi_0$ and to the left of the line $\nu_0(\psi_0) = (\sqrt{2} - 1)\psi_0$.
- To guarantee that all electrons will be gathered by an existing electrode of the collector system $\nu_{c+}(\psi_{0,\min}, \nu_{0,\min}) \geq \nu_{c,\min}$ and $\nu_{c+}(\psi_{0,\max}, \nu_{0,\min}) \geq \nu_{c,\min}$ is required. By visualization this is ensured if the beam rectangle is above the curve $\nu_c = \nu_{c,\min}$ defined by eq. 7. In the example of the figure, $\nu_{c,\min} = 0.4$ and the beam rectangle is above the curve $\nu_c = 0.4$.
- To ensure that the electrons with $\psi_0 > 0$ will be gathered by the appropriate electrode, the inequality $\nu_{c-}(\psi_{0,\max}, \nu_{0,\min}) < \nu_{c,\min}$ should also be satisfied. In other words, the area of the initial beam rectangle in Fig. 3 should not be intersected by the curves with $\nu_c < \nu_{c,\min}$.

An alternative but not optimal definition of the electrode positions simplifies the above constraints and permits a voltage $\nu_{c,\min} = 0$ at the first electrode, independent of the beam energy distribution. In particular, if all the electrodes are placed at the same ψ_c and $-\psi_c$ positions, then the topology of the initial beam properties in the phase space is shown in Fig. 4. Then the constraints are defined as follows: (i) to insert the beam in the decelerating region simply $\psi_{0,\min} > -\psi_c$ and $\psi_{0,\max} < \psi_c$ must be realized, and (ii) to ensure that all electrons are

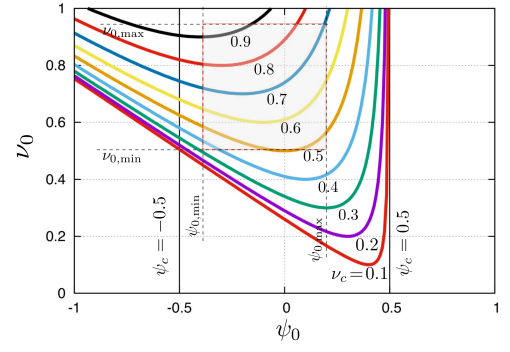


FIG. 4: Phase space of the initial electron beam properties and constraints for the alternative design approach.

gathered by the electrodes the values of $\nu_c(\psi_{0,\min}, \nu_{0,\min})$ and $\nu_c(\psi_{0,\max}, \nu_{0,\min})$ must be real, where the energy of the electrons $\nu_c(\psi_0, \nu_0)$ when their trajectories intersect the electrode surface is given by

$$\nu_c(\psi_0, \nu_0) = \sqrt{-\psi_c^2 + 2(\nu_0 + \psi_0)\psi_c - \psi_0(2\nu_0 + \psi_0)}. \quad (8)$$

Efficiency

The efficiency in both collector approaches is analytically defined. The initial ϵ_{k_i} and the final ϵ_{k_f} kinetic energies of a beam electron at the entrance of the decelerating region and at the position where it is gathered by the electrode, respectively, are written as $\epsilon_{k_i}(\nu_0) = e\Phi_{0,\max} \nu_0^2$ and $\epsilon_{k_f}(\nu_0, \psi_0) = e\Phi_{0,\max} (\nu_0^2 - \nu_c(\nu_0, \psi_0)^2)$. Then, the total initial/final $E_{k,i/f}$ energy of the whole beam is written as

$$E_{k,i/f} = 2\Phi_{0,\max} Y_{\max} \int_{\nu_{0,\min}}^{\nu_{0,\max}} d\nu_0 \int_{\psi_{0,\min}}^{\psi_{0,\max}} d\psi_0 \nu_0 P \epsilon_{k,i/f} \quad (9)$$

where $P = P(\psi_0, \nu_0)$ is the probability density function of the initial energy and Y -position distribution at the entrance of the decelerating region. Then, the collector efficiency is defined by the equation $\eta_c \equiv (E_{k_i} - E_{k_f})/E_{k_f}$. Considering a uniform probability density function the

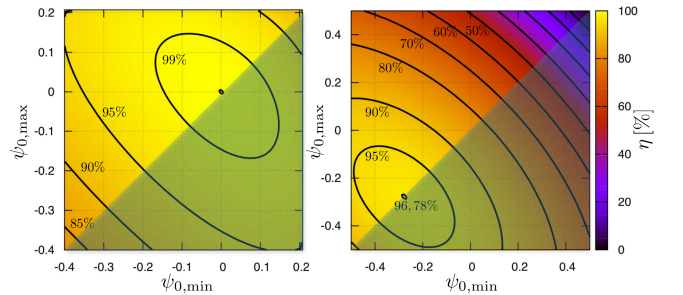


FIG. 5: Efficiency versus $\psi_{0,\min}$ and $\psi_{0,\max}$ of the beam for the optimal (at left) and the alternative (at right) designs.

efficiency can be analytically calculated for both configurations. In Fig. 5, the collector efficiency for all possible values of $\psi_{0,\min}$ and $\psi_{0,\max}$ is plotted in both type of collectors for an initial beam energy in the range of $\nu_{0,\min} = 0.5$ to $\nu_{0,\max} = 1$. In both configuration the efficiency is quite high for an infinitely thin beam: 100 % in the optimal design and 96.78 % in the alternative one. Taking into account also the constraints, the maximum possible beam thickness of the optimal design is $\Delta\psi_0 = 0.6$ with efficiency around $\eta_c \sim 95$ %, while for the alternative design the maximum possible thickness is $\Delta\psi_0 = 1$ with efficiency $\eta_c \sim 73$ %.

In our analysis, an infinite number of electrodes were always considered. This is not the case in the real world where only a small number of electrodes can be used. It is important to estimate the influence of the discrete number of electrodes on the efficiency. Let's suppose that N_e electrodes are used, while $\Phi_{e,i}$ is the applied voltage for electrode i , where $i = 1, \dots, N_e$ and $\Phi_{e,i} > \Phi_{e,i+1}$. Then, all beam electrons, which in the ideal case are gathered by the electrodes with voltages between $\Phi_{e,i}$ and $\Phi_{e,i+1}$, are gathered now by the electrode with voltage $\Phi_{e,i}$. It should be commented here that the shape of the electrodes should ensure that all electrons passing through the gaps will be gathered in order to avoid some stray electrons passing through the electrodes out of the decelerating region. This is considered as a technological issue and it is not further discussed here.

Then, the final kinetic energy of the electron gathered by the electrode with voltage $\nu_{c,i} = (-\Phi_{e,i}/\Phi_{0,\max})^{1/2}$ is written as $\epsilon_{k,f} = \nu_0^2 - \nu_{c,i}^2$ for $\nu_{c,i} \leq \nu_c(\nu_0, \psi_0) < \nu_{c,i+1}$. Then, the total final energy of the beam can be written as

$$E_{k,f} = 2\Phi_{0,\max}Y_{\max} \int_{\psi_{0,\min}}^{\psi_{0,\max}} d\psi_0 \sum_{i=1}^{N_e-1} \int_{\nu(\nu_{c,i};\psi_0)}^{\nu(\nu_{c,i+1};\psi_0)} d\nu_0 P(\nu_0, \psi_0) (\nu_0^2 - \nu_{c,i}^2) \quad (10)$$

where the probability density function $P(\nu_0, \psi_0)$ vanishes for $\nu_0 < \nu_{0,\min}$ and $\nu_0 > \nu_{0,\max}$.

The influence of the collector efficiency as a function of the number of electrodes is analytically calculated for an infinite thin beam with a constant probability density function and supposing that the voltage applied on the

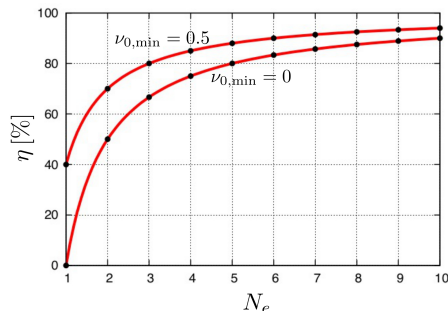


FIG. 6: The dependence of the efficiency on the number of electrodes.

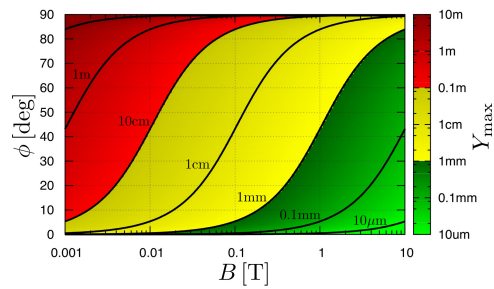


FIG. 7: The dependence of Y_{\max} on the magnetic field B and the angle ϕ for a beam with maximum energy 100 keV.

electrodes in a uniform way, i.e.,

$$\nu_{e,i} = \nu_{0,\min} + (i-1)(\nu_{0,\max} - \nu_{0,\min})/N_e.$$

Then, the collector efficiency is written as

$$\eta = \frac{(N_e - 1)\nu_{0,\max}^2 + (N_e + 1)\nu_{0,\min}^2}{N_e(\nu_{0,\max}^2 + \nu_{0,\min}^2)}. \quad (11)$$

The dependence of the efficiency on the number of electrodes for this case is plotted in Fig. 6 for $\nu_{0,\min} = 0$ and for $\nu_{0,\max} = 0.5$. The first point $N_e = 1$ corresponds to the single stage collector while for $N_e \geq 6$ the efficiency reaches values higher than 80 % and 90 % respectively. In the general case, the energy distribution of the spent beam determines the optimal voltage on the electrodes [14].

Operational range and collector size

The value of the parameter Y_{\max} defined in eq. 5 determines the magnetic field operational range of the proposed MDC design approach and the size of the collector. The optimal position of the electrodes in the y -direction and therefore the size of the collector is determined by the values of this parameter. The dependence of Y_{\max} on the magnetic field B and the angle ϕ is plotted in Fig. 7 for a beam with maximum energy 100 keV.

The yellow region roughly determines a realistic size of such a collector of the order of several millimeters to a few centimeters. In the green region the values of Y_{\max} are too small and the manufacturing tolerances and the stray fields are expected to have strong influence on the operation, while in the red region the values of Y_{\max} are too high and therefore the size of an efficient collector system is too large. Therefore, the proposed design approach could be operated with magnetic fields of a few tens of Gauss using very small angles ϕ up to 1 T using relatively large angles around 80 degrees.

In addition, an important observation of the above analysis is that the axial z -position of the electrodes does not play any role in the operation of such a collector. The electrodes could be placed in a close vicinity to each other. The only limitation is the required isolation and

the voltage standoff stability. Therefore using this approach, very short collectors could be feasible.

III. DESIGN APPROACH FOR GYROTRON ELECTRON BEAMS

The conceptual MDC design presented in Sec. II cannot be directly applied for the collection of the cylindrical hollow electron beam of a conventional gyrotron. This could take place after the transformation of the annular beam to a sheet beam. There are several possible design approaches to achieve this using appropriate magneto-static fields. An indicative idea how to perform this transformation and the application of the design approach proposed in Sec. II is discussed here.

The proposed MDC system has the characteristic that its geometry remains the same along the z -axis. A cross-section of the MDC geometry is shown in Fig. 8. It consists of the central coaxial part in which the hollow cylindrical beam is transformed to a sheet beam and the electron collection section where the deceleration and the collection of the beam electrons take place. The initial position of the beam electrons at the entrance of the collector system is plotted in red. The beam is guided by an externally applied magnetic field B_z which is generated by the main magnet of the gyrotron and some additional coils in the collector region (not shown in Fig. 8). The outer cylinder of the central part is fixed on the top of the mirror box while the inner cylinder is fixed on the top of the collector. Three long normal conducting coils are required for the generation of the appropriate magneto-static field. A coil surrounds the bigger cylinder outwardly while another one is placed internally of the inner cylinder as it is shown in the figure. These two coils can be installed from the top side of the collector and they generate the azimuthal component of the magnetic field in the central part of the collector which guides the beam electrons towards the electron collection section. Dur-

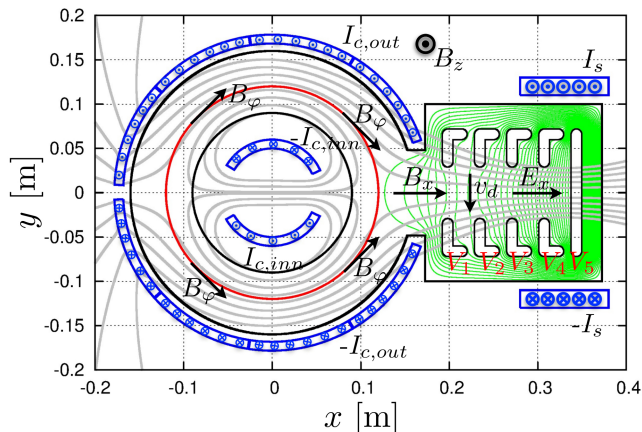


FIG. 8: Cross-section of the MDC conceptual design for gyrotron hollow cylindrical beam.

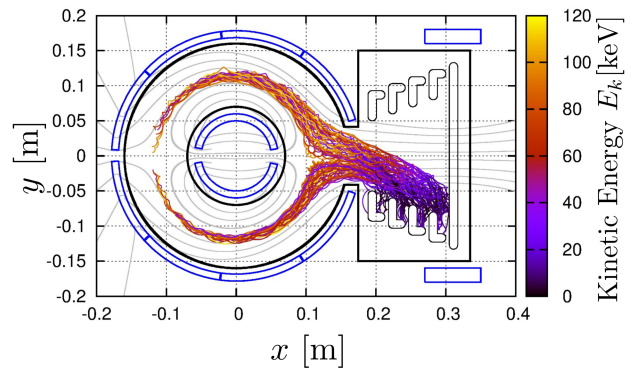


FIG. 9: Trajectories of 100 sample electrons on a preliminary MDC design with five stages.

ing the movement of the electrons along z the azimuthal component of the magnetic field causes a clockwise drift on the electrons with initial azimuthal angles φ between 0 and π and a counterclockwise drift on the electrons with initial φ between 0 and $-\pi$. As a result, all beam electrons will be gradually inserted in the decelerating region between the electrodes along x -axis. A third long stadium shape coil surrounds the electron collection section with the purpose to sustain the sheet beam shape along x -axis.

By this way, the cylindrical hollow beam which moves along z -axis is transformed to a sheet beam moving on the xz -plane at an angle $\phi = \arctan(B_z/B_x)$ compare to the x -axis. The required decelerating electric field E_x along the x -axis is produced by the applied voltage on the electrodes. The drift velocity, given by the equation

$$v_d = \frac{|\mathbf{E} \times \mathbf{B}|}{B^2} = \frac{E_x B_z}{B^2}, \quad (12)$$

pushes the beam electrons to the electrodes placed at the bottom side in Fig. 8.

The projection of the beam trajectories of 100 random sample electrons on the xy -plane in a preliminary optimized geometry are plotted in Fig. 9. Electrons are azimuthally moving towards $\varphi = 0$ without variation of their initial kinetic energy. Then, the electrons are inserted into the deceleration region. Their kinetic energy decreases and in parallel they drift towards the electrodes at the bottom side of the figure. Simulation using the *Ariadne* code with 10000 electrons shown a collector efficiency of 80 % without a significant optimization effort.

The remaining beam current and beam energy along the axial position of the collector is shown in Fig. 10. In order to gather all beam electrons in the specific non-optimum design the length of the collector should be 2.5 m as is shown in the red curves.

A possible idea to shorten the length of the collector is to use more than one beam decelerating section. In this more complicated assembly, three sections are considered while a more complicated system of coils is required. In

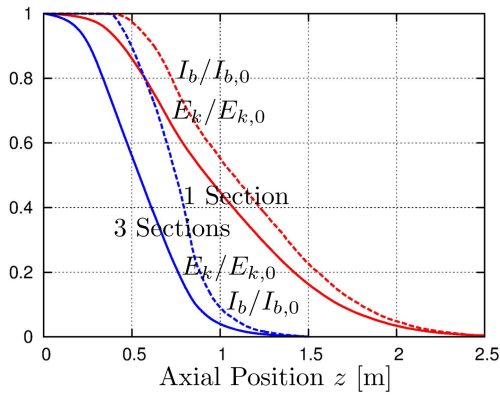


FIG. 10: Normalized beam current and beam energy versus the axial position.

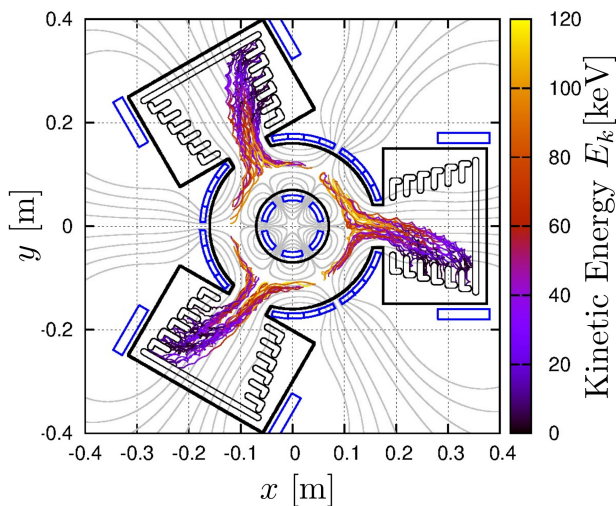


FIG. 11: Trajectories of 100 sample electrons on a preliminary MDC design with seven stages and three collection sections.

parallel, an efficiency higher than 86% was achieved due to the two additional decelerating electrodes used per section. Using this idea, it was possible to shorten the length of the collector to 1.5 m, as shown in Fig. 11. In Fig. 12, the beam cross-section at several axial positions is plotted.

In these simulations initial beam radius and pitch factor distributions have been based on the spent beam of a realistic high power gyrotron [15] while a uniform distribution is considered for the kinetic energy of the electrons at the entrance of the collector system. A two dimensional geometry was considered for the solution of the Laplace equation and the calculation of the electric field while the calculation of the beam trajectories takes place in three-dimensions. The influence of the space charge is not taken into account. In addition, the collector coils are considered to be infinitely long along the z direction. That means that the influence of the bottom and top part of the coils which are necessarily perpendicular to the z -axis is also not considered.

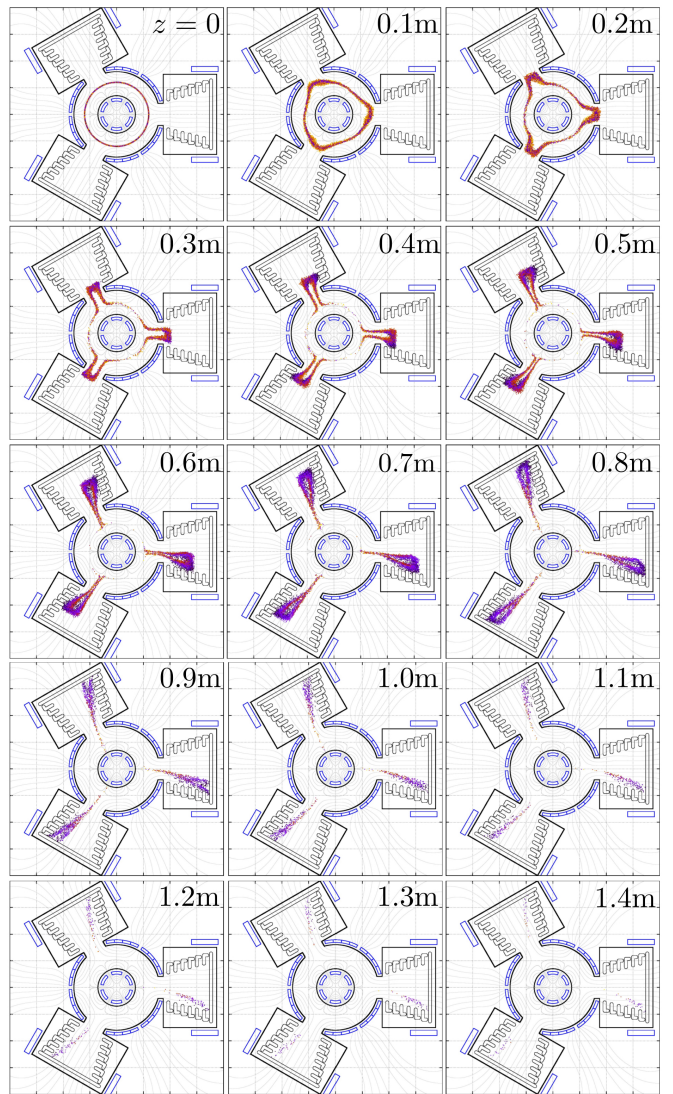


FIG. 12: Beam cross-sections along z in the preliminary MDC system with seven stages and three decelerating sections.

The shape of electrodes, as it was mentioned in Sec.II, should be optimized in order (i) to prevent the beam electrons passing through the electrodes due to $\mathbf{E} \times \mathbf{B}$ drift, (ii) to avoid the slide of the secondary electrons to the neighboring electrodes influencing the overall efficiency and (iii) to keep the electric field between the electrodes in a safe range ensuring the voltage standoff stability. No difficulties are foreseen to optimize the electrode geometry in order achieve that.

A parallel activity has been initiated in which more realistic simulations using the commercial package CST are ongoing. In that work, a realistic geometry of the coils is considered, the influence of the space charge is taken into account and the properties of the spent beam of a high power gyrotron [15] are considered. In the preliminary simulation results a very high efficiency of the order of 85 % with two beam collection sections and seven stages

[14] were also demonstrated. An important issue which should be pointed out is that the level of energy required for the generation of the magnetic field with the normal conducting collector coils in the collector region which is estimated to be of the order of several hundred W. In parallel, the optimization of the shape of the electrodes to satisfy the requirements described above is under investigation.

IV. CONCLUSION

In the first part of the paper, a design approach for the collection of a sheet electron beam is proposed. Based on several considerations, analytical equations have been extracted for the design optimization and the estimation of the collection efficiency. This type of collector is appropriate for devices which operate with a sheet beam confined by a strong magnetic field, such as an FEL or a sheet-beam gyrotron.

In order to apply the proposed design approach to conventional gyrotrons, the transformation of the cylindrical hollow beam to one or more sheet beams is proposed using appropriate magnetostatic fields. A conceptual design for a gyrotron MDC system based on that idea is proposed. In order to illustrate this idea two preliminary slightly-optimized designs were simulated with efficiencies 80 % and 86 %.

The complexity of the electrode geometry is significantly less compared to previous designs based on this concept [9]. However, the manufacturing of such a MDC

system is anyway a technologically challenging problem. In order to answer the question whether this technologically challenging and probably costly approach is attractive or not, the benefits of the use of such a system should be taken into account. Definitely, for low power devices the interest in using such a system is low. However, in fusion reactor ECRH applications where a large number of high power (MW level) and high efficiency CW gyrotrons are required for the generation of microwave power for plasma heating and current drive, such a system could become attractive. In this view, the specifications of the new power supply [16] which is under development in the KIT gyrotron test lab will give us the possibility to test high power gyrotrons with such a MDC system.

V. ACKNOWLEDGMENT

This work has been carried out within the framework of the EUROfusion Consortium and has received funding from the Euratom research and training programme 2014-2018 under grant agreement No 633053. The views and opinions expressed herein do not necessarily reflect those of the European Commission.

The authors would like to warmly thank Prof. I.L. Vomvoridis, Prof. M. Thumm, Dr. B. Piosczyk, Dr. K.A. Avramidis, Dr. G. Gantenbein and M. Schmid for fruitful discussions, V. Rumko for help with designing the figures, Dr. E. Borie for her contribution to the text quality of the manuscript.

-
- [1] M.V. Kartikeyan, E. Borie and M. Thumm, Gyrotrons: high power microwave and millimeter wave technology, Springer, 2003.
 - [2] K. Sakamoto, M. Tsuneoka, A. Kasugai, T. Imai, T. Kariya, K. Hayashi, and Y. Mitsunaka, Major improvement of gyrotron efficiency with beam energy recovery, Physical Review Letters, Vol. 73, Page 3532, 1994.
 - [3] A. Singh, R. L. Ives, R. Schumacher, M. Mizuhara, Multi-stage depressed collector for small orbit gyrotrons, United States Patent, Patent Number 5,780,970, July 1998.
 - [4] A. Singh, S. Rajapatirana, Y. Men, V.L. Granatstein, R.L. Ives, A.J. Antolak, Design of a multistage depressed collector system for 1-MW CW gyrotrons - Part I: Trajectory control of primary and secondary electrons in a two-stage depressed collector, IEEE Trans Plasma Science, vol 27, no 2, pp. 490-502, April 1999.
 - [5] R.L. Ives, A. Singh, M. Mizuhara, R. Schumacher, J. Neilson, M. Gaudreau, J.A. Casey, Design of a multistage depressed collector system for 1-MW CW gyrotrons - Part II: System consideration, IEEE Trans Plasma Science, vol 27, no 2, pp. 503-511, April 1999.
 - [6] S.B. Geer, M.J. Loos, W.H. Urbanus, A.G.A. Verhoeven, 3D design of the fusion-FEM depressed collector using the general particle tracer (GPT) code, Particle Accelerator Conference, New York, 1999.
 - [7] G.P. Saraph, K.L. Felch, J. Feinstein, Ph. Borchard, R. Cauffman, S. Chu, A comparative study of three single-stage, depressed-collector designs for 1-MW, CW Gyrotron, IEEE Trans Plasma Science, vol. 28, no 3, pp. 830-840, June 2000.
 - [8] G. Ling, B. Piosczyk, M.K. Thumm, A new approach for multistage depressed collector for gyrotrons, IEEE Trans Plasma Science, vol 28, no 3, pp. 606-612, June 2000.
 - [9] I.Gr. Pagonakis, J.-Ph. Hogge, S. Alberti, K. A. Avramides, J. L. Vomvoridis, A new concept for the collection of an electron beam configured by an externally applied axial magnetic field, IEEE Transaction on Plasma Science, vol. 36, pp 469-480, 2008.
 - [10] J.P. Hogge, S. Alberti, F. Albajar, P. Benin, S. Bethuys, T. Bonicelli, S. Cirant, E. Droz, O. Dumbrajs, D. Fasel, G. Gantenbein, T.P. Goodman, S. Illy, S. Jawla, J. Jin, S. Kern, C. Lievin, B. Piosczyk, I. Pagonakis, L. Porte, T. Rzesnicki, U. Siravo, M. Thumm, M.Q. Tran, First experimental results from the EU 2 MW coaxial cavity ITER gyrotron prototype, Fusion Science and Technology, Vol. 55, Page 204, 2009.
 - [11] O.I. Louksha, P.A. Trofimov, A method of electron separation for multistep recuperation systems in gyrotrons, Technical Physics Letters, vol. 41, no. 9, pp. 884886,

- 2015.
- [12] T. Okoshi, E. Chiu, Microwave electron tube device, United States Patent, Patent Number 3,526,805, September 1970.
- [13] I. Gr. Pagonakis and J. L. Vomvouridis, The self-consistent 3D trajectory electrostatic code Ariadne for gyrotron beam tunnel simulation, Joint 29th International Conference on Infrared and Millimeter Waves IRMMW and 12th International Conference on Terahertz Electronics, Karlsruhe, Germany, 27 September-1 October, 2004 Conference Digest, Page 657.
- [14] C. Wu, K.A. Avramidis, G. Gantenbein, S. Illy, J. Jelonnek, I.Gr. Pagonakis, M. Thumm, Initial Steps Towards Multi-Stage Collectors for Gyrotrons, 4th ITG International Vacuum Electronics Workshop; Bad Honnef, Germany, 2014.
- [15] I. Gr. Pagonakis, F. Albajar, S. Alberti, K. Avramidis, T. Bonicelli, F. Braumueller, A. Bruschi, I. Chelis, F. Cismondi, G. Gantenbein, V. Hermann, K. Hesch, J.-P. Hogge, J. Jelonnek, J. Jin, S. Illy, Z. Ioannidis, T. Kobarg, G. Latsas, F. Legrand, M. Lontano, B. Piosczyk, Y. Rozier, T. Rzesnicki, C. Schlatter, M. Thumm, I. Tigelis, M.Q. Tran, T.-M. Tran, J. Weggen, J.L. Vomvouridis, Status of the development of the EU 170 GHz/1 MW/CW gyrotron, Fusion Engineering and Design, <http://dx.doi.org/10.1016/j.fusengdes.2015.02.050>, 2015.
- [16] M.6. M. Schmid, J. Franck, P. Kalaria, K. A. Avramidis, G. Gantenbein, S. Illy, J. Jelonnek, I. Gr. Pagonakis, T. Rzesnicki, M. Thumm, Gyrotron Development at KIT: FULGOR Test Facility and Gyrotron Concepts for DEMO, Fusion Engineering and Design, Vol. 96-97, Page 589, 2015.[doi:10.1016/j.fusengdes.2015.03.003](http://dx.doi.org/10.1016/j.fusengdes.2015.03.003)